Delayed compression and breakage of crushed mudstones due to the drying/wetting and temperature cycles

Mohamed Nihaaj [1], *Takashi* Kiyota [1], *Masataka* Shiga [1] and *Toshihiko* Katagiri [1]

[1] *Institute of Industrial Science, University of Tokyo, Japan*
[#]*Corresponding author: nihaaj@iis.u-tokyo.ac.jp*

ABSTRACT

Soft sedimentary rocks, especially mudstones, disintegrated or crumbled when subjected to cyclic drying and wetting, known as slaking, which was the cause of severe slope failures and ground settlement. Drying/wetting and temperature variation are the influential factors of the slaking. In this study, a conventional oedometer was modified to make a drying/wetting cycle with temperature variation to examine the effects of slaking for four materials with different slaking ratios. Further, one of the four materials (Hamamatsu mudstone), showing higher vertical strains along the drying/wetting cycle, was experimented with under three loading conditions (100 kPa, 200kPa & 500 kPa) and drying/wetting cycles, in which the particle breakage was also measured along the drying/wetting cycles. In addition, a needle penetration test was conducted along the drying/wetting cycles. In the continuous drying/wetting cycles, the occurrence of particle breakage was higher in lower-stress conditions, where the void ratio became a governing factor for the breakage over vertical stress. The needle penetration resistance is dependent on two factors which are density and particle size, and there was a trade-off between them along the drying/wetting cycles. After a couple of drying/wetting cycles, the particle crushing resulted in a noticeable reduction in penetration resistance in lower stress conditions.

Keywords: Slaking; Oedometer test; Slaking; Particle breakage; Penetration resistance.

1. Introduction

Representing no less 35% of the earth's crust, clay-bearing rock degrades its strength once disturbed or exposed to weathering (Franklin et al.1972). So, there is a need for greater attention to be paid to long terms behaviours of such sedimentary rocks (Kikumoto et al. 2016).

Tertiary mudstone deposits with slaking nature extensively cover Japan's coastal and mountainous areas and are the most often encountered geologic material in excavation (Yoshida et al. 2002). Thus, considering environmental and economic issues, it has been suggested to use mudstones as a construction material, particularly for earth structures or filling.

The strength and deformation characteristics of soft rocks, especially mudstone, deteriorate when the material is exposed to drying/wetting cycles, known as slaking, which was the cause of severe slope failures and ground settlements in several case studies (Nakano 1967; Takagi et al. 2010; Yagiz 2011). Further, some residential buildings built on the mudstone filling were tilted by differential settlement, caused by particle breakage and slaking (Mochizuki et al. 1985).

The effect of temperature variation in clay material at one-dimensional compression has been observed by several researchers (Paaswell 1967; Towhata et al. 1993). Moreover, the coupling effect of the drying/wetting with temperature (higher temperature in drying and lower temperature in wetting) caused a severe effect on volume changes in slaking material, as observed by Zhang et al. (2015, 2012). However, the literature does not comprehensively discuss particle breakage and vertical strain along the drying/wetting cycles with temperature variation.

Therefore, this research targets to investigate the coupling effect of slaking, caused by drying/wetting with temperature variations cycle, on one-dimensional deformation, particle breakage, and needle penetration resistance. A modified oedometer apparatus was developed to apply a cycle of drying/wetting with temperature changes on a sample.

2. Material

The gravelly mudstones used in this study were collected from several sites at Shizuoka, and Okinawa Prefectures in Japan, and Hattian Bala in Pakistan. For comparison, a non-slaking gravel material was also used. The physical properties of the tested materials are shown in Table 1.

Slaking ratio, as mentioned in Table 1, was measured according to the Japanese highway standard (JHS110-2015), here in this Test, a 300-g dry specimen (with a particle size of 19.5–37.5 mm) underwent one cycle of drying (24 h) followed by immersion (24h). Then, the dry mass of the specimen was sieved by a 9.5-mm sieve; the percentage of the dry weight of passing the material through that sieve was defined as the slaking ratio.

Table 1. Four different materials' physical properties

Material	Slaking index (JGS,2124)	Slaking durability (ASTM D4544, 2016)		Slake ratio (%) (JHS110-2015)	Specific density (g/cm3)	Max ρdmax (g/cm3)	Wabs (%)
		Id 1 (%)	Id 2 (%)				
Ham	3	92.13	73.75	55.50	2.690	1.65	12.7
Oki	4	81.25	61.21	73.71	2.650	1.39	45.0
HB	2	99.35	98.59	3.10	2.780	1.74	3.0
NSG	0	100.00	100.00	0.00	2.702	1.91	0.6

The collected samples were crumbled into relatively smaller particles to increase the surface area (so as to accelerate the slaking) and reduce the specimen's height: maximum particle size ratio to avoid arch formation (Mokhtari et al. 2015). Since very smaller particles are resistant to slaking as observed by Qi et al. (2015), the initial particle was kept between 2.00 to 4.75 mm as suggested by Kiyota et al. (2011) and Sharma et al. (2017).

Dry specimens, with a diameter, ϕ=150mm and height, h=150mm, were prepared into the mould in five layers. To avoid particle breakage during sample preparation, compaction was only done by the external vibration (Kiyota et al. 2011), which was calibrated to maintain the compaction degree (Dc) of 78-80% of Hamamatsu mudstone (lower density was kept to increase the water saturation and slaking). Anyhow compaction energy was kept constant for all specimens. For further details, refer to Nihaaj et al. (2021). Different types of mudstones were compacted at different degrees at a given compaction energy because of their varying compaction properties. The maximum dry densities of the mudstones were explained in Table 1 as max ρ_{dmax}.

3. Apparatus and test procedures

3.1. Modified oedometer test

To investigate the one-dimensional deformation characteristics of gravelly mudstone subjected to drying/wetting cycles, a modified oedometer apparatus was developed. The schematic diagram and laboratory set-up of the modified oedometer are shown in Fig. 1(a) & (b) respectively. The modified oedometer apparatus is an oedometer (ϕ=150 mm and h=150 mm), additionally consisting of a drying/wetting system.

3.2. Drying/wetting system

A water tank was connected to the bottom of the specimen (through valve No 1), and water was allowed to flow upward into the specimen to wet the specimen until the vertical strain was settled (which was calibrated as 6 hours). Subsequently, the drying was done by allowing water to drain through valve No.3, wrapping a heater around the specimen mould, and circulating dry air into the specimen (through valve No 4 to No 3). A thermometer was inserted inside the specimen for calibration, and the heater's temperature was changed (at the outer surface). An average specimen temperature of 56 °C was achieved by controlling the outer surface temperature during the drying stage, which was limited to 56 °C to avoid any unrealistic chemical reaction in the sample (Zhang et al. 2012). The vertical strain was continuously measured by an External Displacement Transducer (EDT). Time for drying up to less than 1% of moisture content was calibrated (as 48 hours) by inserting a moisture sensor into the mold, and the calibration curve of three different materials (water content reduction vs. time) was presented in Fig. 1(c) This comprehensive dry and wet cycle (6 hours wetting and 48 hours drying as mentioned earlier) hereinafter is referred to as the D/W cycle in this paper).

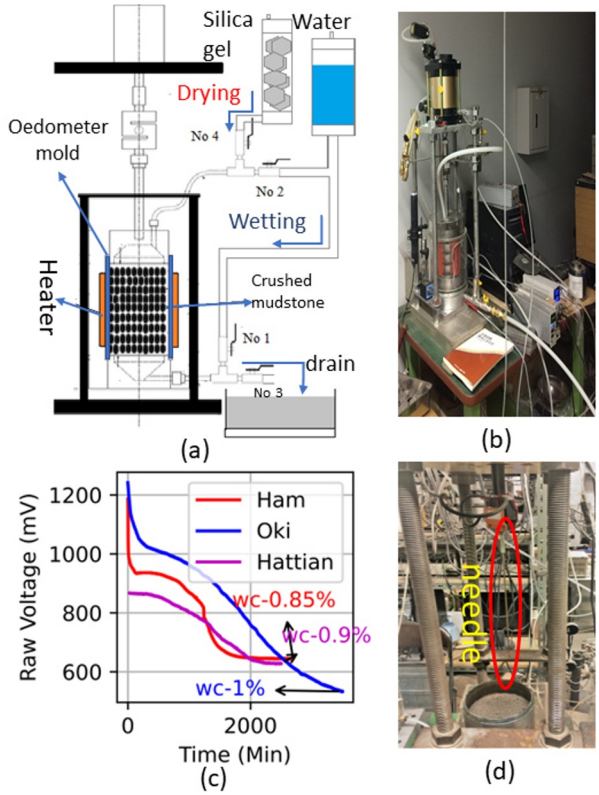

Figure 1. (a) Schematic diagram, (b) laboratory setup of Modified oedometer, (c) Raw voltage/water content (%) vs. time at calibration, and (d) laboratory setup of the needle penetration test.

4. Experimental set-up

4.1. Oedometer test

Table 2 explains the tested Four specimens, H-200-9, OKI-200-9, HB-200-9, and NSG-200-9, which were prepared using four materials: Hamamatsu mudstone, Okinawa mudstone, Hattian Bala mudstone, and non-slaking gravel respectively. First, these four specimens were subjected to 200 kPa vertical stress (σ_v) and 9 D/W cycles in the modified oedometer. Then, this series of experiments was extended for another two vertical stress conditions (100, and 500 kPa) for Hamamatsu mudstone. The details of this series are summarized in Table 2.

Table 2. Experimental set-up of Oedometer

Sample name	Degree of comp (Dc)	σv (kPa)	D/W cycle	Note
H-200-9	78	200	9	Br/Pen
HB-200-9	85	200	9	
OKI-200-9	78	200	9	
NSG-200-9	92	200	9	
H-100-9	78	100	9	Br/Pen
H-500-9	78	500	9	Br/Pen
H-100-0	78	100	0	Br
H-200-0	78	200	0	Br
H-500-0	78	500	0	Br
H-100-1	78	100	1	Br/Pen
H-200-1	78	200	1	Br/Pen
H-500-1	78	500	1	Br/Pen
H-100-3	78	100	3	Br
H-200-3	78	200	3	Br
H-500-3	78	500	3	Br
H-100-5	78	100	5	Br/Pen
H-200-5	78	200	5	Br/Pen
H-500-5	78	500	5	Br/Pen

Br- After the D/W cycle, the specimen was sieved, and Relative Breakage (Br) was calculated
Pen- Needle penetration test conducted.
Dc- Degree of compaction

4.2. Needle Penetration test

The laboratory setup of the needle penetration test is illustrated in Fig. 1(c) and was carried out to evaluate the effect of the D/W cycles on the strength characteristics of the specimen, which were tabulated in Table 2 (penetration resistance measured samples are indicated as Pen in the Note column). Needle penetration was done after completing a particular D/W cycle at constant vertical stress to minimize the vertical stress influence.

The penetration resistance and penetration depth were monitored by a load cell and an EDT, respectively. A metal stick with a diameter of 3 mm, 60^0 apex angle, and a length of 150 mm was mounted below the load cell. The mould: stick diameter ratio was kept at 50 to reduce the rigid boundary effect that could be caused by stiff oedometer mould (Pournaghiazar et al. 2011; Monfared 2014). The penetration test was done at 0.15 mm/sec, lower than ASTM D5778-2012 requirement, where the allowable is 20 mm/s, to reduce the particle size effect (Kokusho et al. 2003). The penetration test was done to an approximate depth of 100 mm from the top. The results are intended to represent the penetration strength qualitatively, along with the D/W cycles.

4.3. Particle breakage

In the oedometer test, the particle breakage is impossible to be measured along the D/W cycle. So, a number of the specimen were prepared by using Hamamatsu mudstone in the same initial conditions, on that different D/W cycles (0, 1,3, 5, & 9) in different vertical stress conditions (100, 200 & 500 kPa) were applied. At the end of the respective cycles, the remaining material in the mould was sieved to calculate the particle breakage. This experiment's conditions were explained in Table 2 as Br in the Note column. After the respective D/W cycles, the relative particle breakage index (Br), proposed by Hardin (1985), was evaluated.

5. Test results

5.1. Oedometer test

Fig. 2 (a) illustrates the vertical strain (ε_v) changes of four different materials at the 200 kPa vertical stress conditions. In Fig. 2(a), the hollow circles represent the dried and heated states (56 °C), whereas the solid circles represent the wetted state at 20^0C. However, minor variations in the strain were also observed during the drying and wetting state because wetting and drying are related to the swelling and contraction behaviour respectively. The swelling is caused by water absorption of the mudstones. The contraction, caused by drying, is explained and related to the shrinkage of macro and micro pores by Sharma et al. (2017).

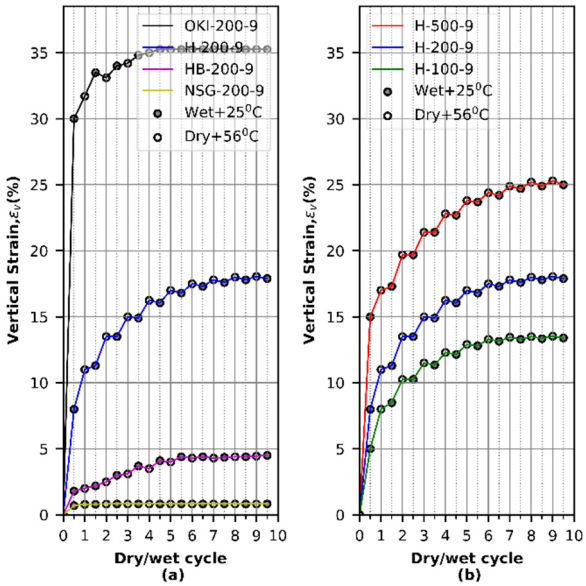

Figure 2. Vertical strain (ε_v) vs. D/W- cycle of (a) four different mudstones at 200 kPa vertical stress, and (b) Hamamatsu mudstone at different vertical stress.

The Okinawa (OKI-200-9) and Hamamatsu (H-200-9) mudstone showed more significant vertical strain (ε_v) development along the D/W cycle, up to 35% and 17.5%, respectively, compared with the other specimens prepared using Hattian Bala (HB-200-9) or non-slakable gravel (NSG-200-9), showing the vertical strain (ε_v) less than 5% at the end of the 9^{th} cycle.

Both, OKI-200-9 and H-200-9, showed severe increment at the first wetting due to the dried and pebble state of the initial condition and collapse behaviour, it is further explained by Oldecop et al. (2001) that compression at the initial stage develops micro-cracks in gravelly mudstone, that lead to the breakage once it was exposed to wetting. Anyhow the increment in vertical strain (ε_v), caused by subsequent D/W cycles, was

reduced along the D/W cycles and became flat after a few D/W cycles.

Fig. 2(b) explains the vertical strain (ε_v) changes of the Hamamatsu mudstone under the three different vertical stress conditions (σ_v =100, 200, and 500 kPa). The first wetting caused a large ε_v, which increases along the increment of vertical stress (σ_v).

However, minor variations in vertical strain (ε_v) were also observed during the drying and wetting state because wetting and drying showed swelling and contraction behaviour, respectively. After the 8th cycle, none of these stress conditions further showed vertical strain (ε_v) development.

Figs. 3(a), (b), and (c) show the particle gradation curves of the samples after the loading, 1,3, 5 and 9 D/W cycle subjected to σv=100, 200 and 500 kPa vertical stress conditions respectively, testing conditions of which is explained in Table 2. Particle breakage increases along the D/W cycles irrespective of their vertical stress conditions.

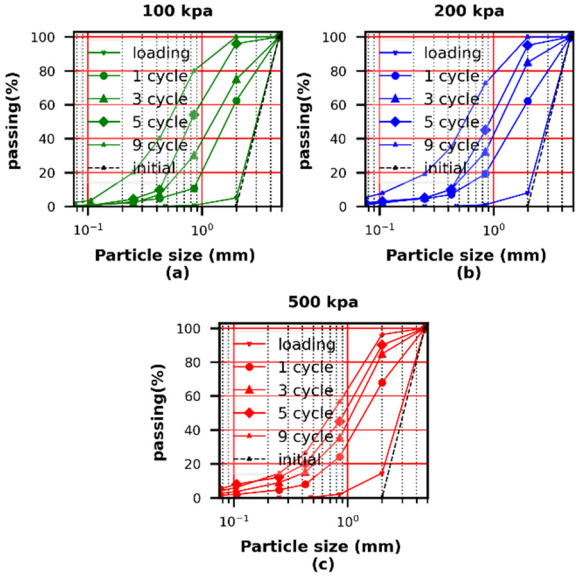

Figure 3. Particle gradation of the sample subjected to (a) σ_v=100kPa, (b) σ_v=200kPa, and (c) σ_v=500kPa, along D/W-cycle.

5.2. Penetration resistance

Figs. 4 (a), (b), and (c) show the penetration resistance along the depth of the specimen of Hamamatsu mudstone after the 1st, 5th, and 9th D/W cycles in 100, 200, and 500 kPa vertical stress conditions, respectively. The penetration resistance increased with the depth due to the increased confinement and the needle's surface area exposed to soil friction in all stress conditions. Furthermore, the resistance increased with increasing D/W cycles due to the densification until the 5th D/W cycle in all vertical stress conditions. However, an increment in penetration resistance after the 9th D/W cycle was only observed in 500 kPa condition (H-500-9 in Fig. 4(c)) than respective 5th D/W cycles (H-500-5 in Fig. 4(c)). Conversely, penetration resistance of the 9th D/W cycle at 100 and 200 kPa vertical stress conditions (H-100-9 and H-200-9 in Figs. 4(a) and (b), respectively) did not show any apparent increases compared with the respective 5th D/W cycle (H-100-5 and H-200-5 in Figs. 4(a) and (b) respectively).

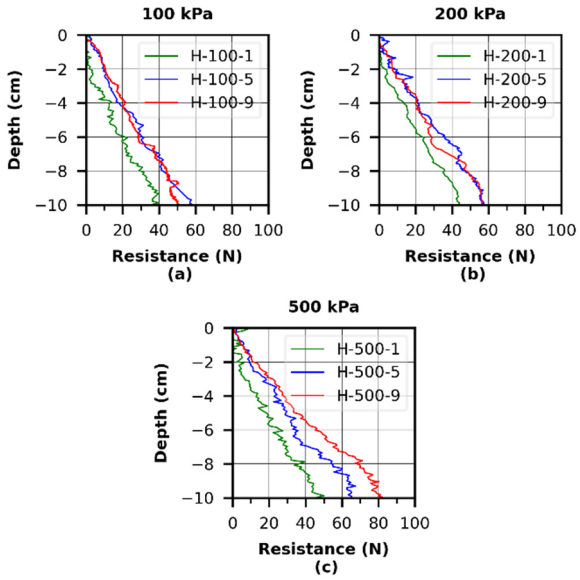

Figure 4. Penetration resistance of (a)100 kPa, (b) 200 kPa, and (c) 500 kPa after 1st,5th, and 9th D/W-cycle.

5.3. Particle breakage

Fig. 5(a) shows the relative particle breakage (Br) (quantified by Hardin (1985)) of the samples after the loading (0-cycle), 1st,3rd, 5th, and 9th D/W-cycles under various σ_v conditions, as per explained in Table 2 and Fig 3. The Br increased along with the increment of the D/W cycles in all samples. After the 1st D/W cycle, the Br at 500 kPa stress condition is higher than other stress conditions (100 and 200 kPa).

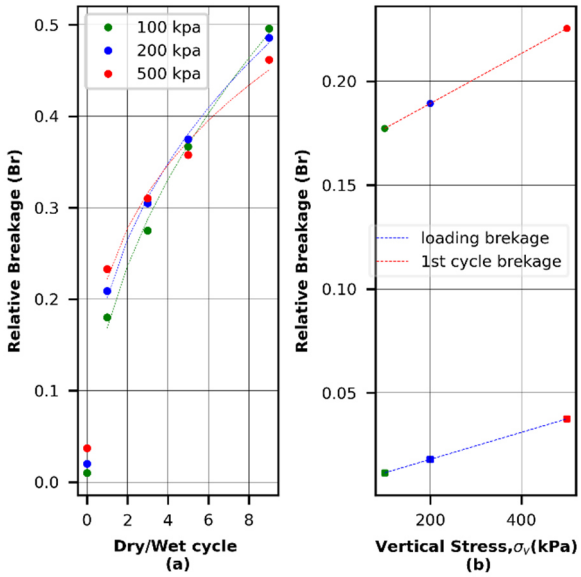

Figure 5. (a) Relationship of Relative Breakage (Br) vs. the D/W cycle, (b) Relationship breakage vs. vertical stress at loading and 1st D/W cycle

However, after the 5th and 9th D/W cycles, the 500 kPa stress sample showed lower Br. Conversely, the lower stress condition (100 kPa) showed lower Br after the 1st D/W cycle but higher Br at the 9th D/W cycle.

Fig. 5(b) explains the Br after loading and the 1st D/W cycle, where the Br and the vertical stress (σ_v) show a linear relationship. Figs. 6(a) and (b) explains particle arrangement before and after the 1st D/W cycle, respectively.

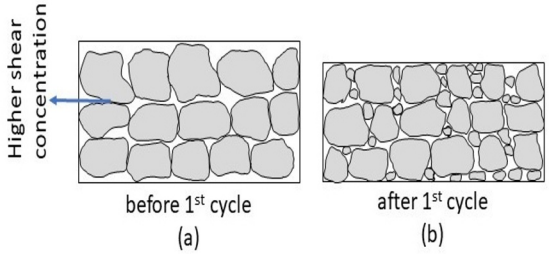

Figure 6. Particle arrangement (a) Before 1st D/W cycle and (b) After 1st D/W cycle

6. Discussion

The specimen was prepared by dry and crushed gravelly mudstone, in an extremely looser state, and this sort of void condition is impossible to exist in real cases and above the normally consolidated line (Nakano et al. 1998). The increment of vertical stress (σ_v) increases the finer particles as shown in Fig. 3, those fine particles could be accommodated into the voids in between the loosely packed gravelly mudstones. Thus, this sort of breakage pattern in gravelly mudstones does not increase the coordination numbers (particle contacts), as expected in the granular specimen, within the tested vertical stress (σ_v) range. That would be a reason for showing a linear relationship between vertical stress (σ_v) and Br in Fig. 5(b), the same sort of linear relation between vertical stress and Br was found in the same type of slaking material in other literature (Zhang et al. 2012).

Even though the specimen was loaded in a one-dimensional condition, shear stress concentration could be developed in particle contact as per Fig. 6(a) At the initial condition, shear stress concentration at the particle contact was high due to the initial lower density and narrow range of particle size (2-4.75mm) (lower particle contact). Therefore, the surface of the particles can be softened due to swelling at the wetting state, as observed in heavily over-consolidated clays, which causes severe breakage (Nakano et al. 1998). So vertical stress (σ_v) and shear concentration in between the particles are the governing factors on the increment of breakage at the first cycle. Therefore, the vertical stress (σ_v) and increment of breakage showed a linear relation in Fig. 5(b).

As per Nakano et al. (1998), this phenomenon of shear concentration is not significant at a denser state, where the number of contact increases and the shear concentration is significantly reduced, as per illustrated in Fig 6.(b). Thus, voids became the governing factor over the shear stress concentration along the D/W cycles. An increment in voids increases the degree of slaking in the particle (Dick et al. 1992), which causes particle breakage in continuing D/W cycle. Thus, under 100kPa the increase in Br, because of the higher void, is greater than the higher loading condition (500kPa).

Fig. 7 explains the increment of the Br after the first cycle (2 to 9 D/W cycles). Increment of particle breakage could be influenced by vertical stress (σ_v) and void (e) of the specimen; thus, three trends in Fig. 7 could be observed with the vertical stress (σ_v) conditions. The void ratio reduction was increased severely in higher stress conditions resulting in lower breakage increment in continuing D/W cycles.

The penetration resistance of the miniature rods is influenced by density and particle size (George et al. 2003). An increase in density and particle size could increase the penetration resistance. Fig. 8 shows the relationship between the vertical strain (ε_v) and the Br in all stress conditions. Along the D/W cycle, the Br exponentially increased over vertical strain (ε_v). This exponential increment was very high in the lower vertical stress conditions (100 and 200 kPa) than in the higher stress condition (500 kPa). Even though the particle size was reduced along the D/W cycle due to the breakage, specimen density was increased due to increasing vertical strain (as per Fig. 8). Increasing density is the governing factor rather than reducing particle size in the penetration resistance up to the 5th D/W cycle.

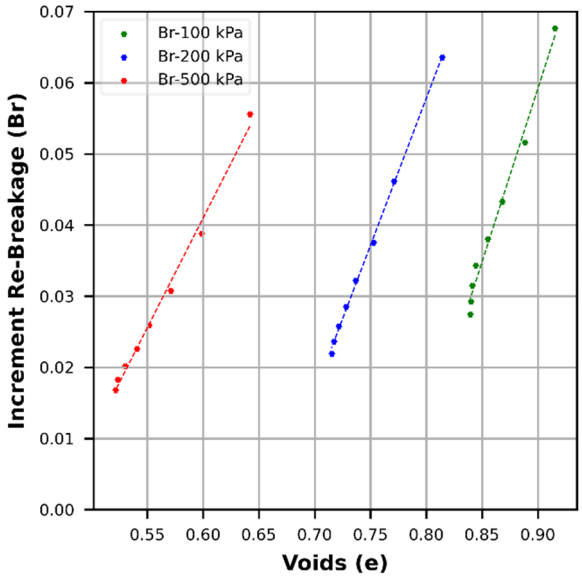

Figure 7. Relationship of increment of breakage vs. voids at continuing D/W cycle (2 to 9 D/W cycle).

The vertical strain (ε_v) did not increase in lower vertical stress conditions (100 and 200 kPa) after the 5th D/W cycle, as shown in Fig.8. Thus, the influence of the density increment was severely limited in lower stress conditions (100 and 200 kPa), which decreased the penetration resistance at the 9th D/W cycle (Fig. 3 (a)-H-100-9 and Fig. 3 (b)-H-200-9). But the higher vertical stress condition (500 kPa) showed substantial increases in the vertical strain (ε_v) (density) up to the 9th D/W cycle. So, the penetration resistance of the 9th cycle at the higher vertical stress (Fig. 5 H-500-9) has shown an increment in penetration resistance.

7. Conclusions

The modified oedometer test was conducted to evaluate the vertical strain (ε_v) among the mudstones with different physical properties along the D/W cycle. The results showed a severe increment of vertical strain (ε_v) in the material with a higher slaking ratio. The particle breakage (Br) along the D/W cycle depended on two factors, vertical stress and voids. In the first D/W cycle,

vertical stress was the governing parameter. However, at continuing the D/W cycle, voids became the governing factor. The penetration resistance depended on two factors, density and particle size. At continuing D/W-cycle, there was a trade-off between density and particle size.

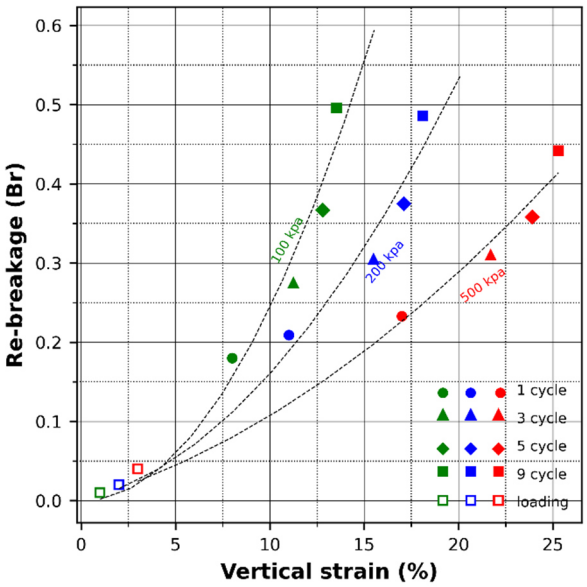

Figure 8. Relationship of Vertical strain (ε_v) (%) vs. Relative Breakage (Br) in different vertical stress.

Reference

ASTM, A. S. T. M. 2016. "Standard Test Method for Slake Durability of Shales and Other Similar Weak Rocks.", *ASTM international*. http://doi: 10.1520/D4644-16.

Dick, J. C. and Shakoor, A. 1992. "Lithological controls of mudrock durability." *Quarterly Journal of Engineering Geology*, 25(1), pp. 31–46. http://doi: 10.1144/gsl.qjeg.1992.025.01.03.

Franklin, J. A. and Chandra, R. (1972). "The slake-durability test." *International Journal of Rock Mechanics and Mining Sciences and*, 9(3), pp. 325–328. http://doi: 10.1016/0148-9062(72)90001-0.

Anagnostopoulos, A., Koukis, G., Sabatakakis, N. and Tsiambaos, G., 2003. "Empirical correlations of soil parameters based on cone penetration tests (CPT) for Greek soils." *Geotechnical & geological engineering*, *21*, pp.377-387.

Kikumoto, M., Putra, A. D. and Fukuda, T. 2016. "Slaking and deformation behaviour." *Geotechnique*, 66(9), pp. 771–785. http://doi: 10.1680/jgeot.15.P.285.

Kiyota, T., Sattar, A., Konagai, K., Kazmi, Z.A., Okuno, D. and Ikeda, T., 2011. "Breaching failure of a huge landslide dam formed by the 2005 Kashmir earthquake." *Soils and foundations*, *51*(6), pp.1179-1190.

Kokusho, T., Murahata, K., Hushikida, T. and Ito, N., 2003. "Introduction of miniature cone in triaxial apparatus and correlation with liquefaction strength.". In Proc. of Annual Convention of JSCE (Vol. 3, No. 96, pp. 191-192).

Mochizuki, A., Mikasa, M. and Kawamoto, S., 1985. "Investigation of settlement of clay fill at a housing development site." Tsuchi-To-Kiso, 33(4), pp.25-32.

Mokhtari, M., Shariatmadari, N., Heshmati R, A.A. and Salehzadeh, H., 2015." Design and fabrication of a large-scale oedometer." Journal of Central South University, 22, pp.931-936.

Monfared, S.D., 2014. Miniature Cone Penetration Test on Loose Sand. The University of Western Ontario (Canada).

Nakano, R., 1967. "On weathering and change of properties of tertiary mudstone related to landslide." Soils and Foundations, 7(1), pp.1-14.

Nihaaj, N.M., Kiyota, T. and Chua, M.G., 2022. "Internal erosion of gravelly mudstone due to drying–wetting and hydraulic pressure cycles in oedometer test." Canadian Geotechnical Journal, 59(7), pp.1299-1303.

Hardin, B.O., 1985. "Crushing of soil particles. Journal of geotechnical engineering." 111(10), pp.1177-1192.

Oldecop, L.A. and Alonso, E.E., 2001. "A model for rockfill compressibility." Géotechnique, 51(2), pp.127-139.

Paaswell, R. E. 1967 "Temperature Effects on Clay Soil Consolidation", *Journal of the Soil Mechanics and Foundations Division*, 93(3), pp. 9–22.

Pournaghiazar, M., Russell, A. R. and Khalili, N. 2011 "Development of a new calibration chamber for conducting cone penetration tests in unsaturated soils." *Canadian Geotechnical Journal*, 48(2), pp. 314–321. http://doi: 10.1139/T10-056.

Qi, J., Sui, W., Liu, Y. and Zhang, D., 2015. "Slaking process and mechanisms under static wetting and drying cycles slaking tests in a red strata mudstone." Geotechnical and Geological Engineering, 33, pp.959-972.

Sharma, K., Kiyota, T. and Kyokawa, H. 2017. "Effect of slaking on direct shear behaviour of crushed mudstones.", *Soils and Foundations*. Japanese Geotechnical Society, 57(2), pp. 288–300. http://doi: 10.1016/j.sandf.2017.03.006.

Takagi, M., Yokata, S., Suga, K., Yasoda, S. and Ota, H., 2010. "The actual situation of the slope of earthfill that collapsed by an earthquake disaster in the Tomei Expressway Makinohara district." In Journal of Geotechnical Engineering Symposium, JGS (Vol. 55, No. 29, pp. 193-196).

Towhata, I., Kuntiwattanaku, P., Seko, I. and Ohishi, K., 1993. "Volume change of clays induced by heating as observed in consolidation tests. soils and foundations." 33(4), pp.170-183.

Yagiz, S. 2011 "Correlation between slake durability and rock properties for some carbonate rocks.", *Bulletin of Engineering Geology and the Environment*, 70(3), pp. 377–383. http://doi: 10.1007/s10064-010-0317-8.

Yoshida, N., Enami, K. and Hosokawa, K. 2002. "Staged compression-immersion direct shear test on compacted crushed mudstone.", *Journal of Testing and Evaluation*, 30(3), pp. 239–244. http://doi: 10.1520/jte12311j.

Zhang, B. Y., Zhang, J. H. and Sun, G. L. 2012. "Particle breakage of argillaceous siltstone subjected to stresses and weathering.", *Engineering Geology*. Elsevier B.V., 137–138, pp. 21–28. http://doi: 10.1016/j.enggeo.2012.03.009.